THE JOURNAL OF BIOLOGICAL CHEMISTRY
Vol. 275, No. 49, Issue of December 8, pp. 38494–38499, 2000

Printed in U.S.A.

X-ray Structures of the Apo and MgATP-bound States of *Dictyostelium discoideum* Myosin Motor Domain*

Received for publication, June 26, 2000, and in revised form, August 18, 2000
Published, JBC Papers in Press, August 22, 2000, DOI 10.1074/jbc.M005585200

Cary B. Bauer, Hazel M. Holden, James B. Thoden, Robert Smith, and Ivan Rayment‡

From the Department of Biochemistry, University of Wisconsin, Madison, Wisconsin 53706-1544

Myosin is the most comprehensively studied molecular motor that converts energy from the hydrolysis of MgATP into directed movement. Its motile cycle consists of a sequential series of interactions between myosin, actin, MgATP, and the products of hydrolysis, where the affinity of myosin for actin is modulated by the nature of the nucleotide bound in the active site. The first step in the contractile cycle occurs when ATP binds to actomyosin and releases myosin from the complex. We report here the structure of the motor domain of *Dictyostelium discoideum* myosin II both in its nucleotide-free state and complexed with MgATP. The structure with MgATP was obtained by soaking the crystals in substrate. These structures reveal that both the apo form and the MgATP complex are very similar to those previously seen with MgATPγS and MgAMP-PNP. Moreover, these structures are similar to that of chicken skeletal myosin subfragment-1. The crystallized protein is enzymatically active in solution, indicating that the conformation of myosin observed in chicken skeletal myosin subfragment-1 is unable to hydrolyze ATP and most likely represents the pre-hydrolysis structure for the myosin head that occurs after release from actin.

Directed movement is one of the features common to living organisms. This property is provided by a suite of molecular motors that includes, myosin, dyenin, and kinesin in eukaryotes and bacterial flagella motors in prokaryotes. In each molecular motor the energy to drive this process is derived from the hydrolysis of ATP. For all of these motors, it has long been suspected that conformational changes associated with differential affinity of the motor protein for ATP and its hydrolysis products are responsible for energy transduction. After many years of study, it has proved to be difficult to identify the nature of the conformational changes that underlie directed movement, with the exception of myosin. However, even with myosin important questions remain.

Myosin is the most abundant and best known molecular motor. Although initially identified in skeletal muscle, isoforms of this protein have been observed in all eukaryotic cells where it fulfills a wide range of cellular functions from muscle contraction, cellular locomotion, and chemotaxis to organelle transport (1, 2). Indeed over 15 classes of myosin have now been identified. All of these proteins contain a section of their sequence that can be associated with a motor domain. The catalytic cycle of myosin reveals at first sight a counterintuitive relationship between the chemical step of hydrolysis and the energy transduction process. In myosin the energy transduction step is associated with product release rather than ATP hydrolysis.

Kinetics studies have revealed that in the absence of ATP, myosin binds very tightly to actin to form the rigor state. Upon addition of ATP, myosin rapidly changes to a weakly bound state prior to nucleotide hydrolysis. Thereafter ATP is rapidly hydrolyzed, but the hydrolysis products remain tightly bound to myosin. Rebinding to actin catalyzes the release of inorganic phosphate and triggers the start of the powerstroke (3, 4). Spectroscopic and fiber diffraction studies have shown that conformational changes in the myosin motor domain and its attached light chains are intimately involved in the energy transduction step (5–8). A full molecular understanding of this biological process requires a detailed structural view of each of the distinct states of the contractile cycle.

The structure of myosin has been determined for four organisms in a range of conformations. These include chicken skeletal myosin subfragment-1 with sulfate in the active site (9), *Dictyostelium discoideum* myosin II truncated head (S1dC)[1] with a variety of nucleotides bound in the active site (10–15), smooth muscle myosin head with its essential light chain and the smooth muscle motor domain (16), and scallop myosin S1 (17). A question inherent to all of these structures is their relationship to the conformational states that are transitioned through or populated within the contractile cycle.

The first structure for myosin subfragment-1 was that of chicken skeletal myosin subfragment-1 (9). This protein was crystallized from ammonium sulfate in the absence of nucleotide and was observed to contain a sulfate ion bound in the P-loop. Because this was the first determined structure, it was unknown where this structure belonged in the catalytic cycle. Initially, it was believed to represent a point after release from actin but prior to formation of the metastable state (18). However because the overall structure seemed to fit a reasonable model for the actomyosin complex based on image reconstructions it was subsequently ascribed by Holmes (19) to the rigor state. Subsequent studies on a truncated myosin head or motor domain from *D. discoideum* revealed two conformations, one of

* This research was supported by National Institutes of Health Grant AR35186 (to I. R). The costs of publication of this article were defrayed in part by the payment of page charges. This article must therefore be hereby marked "*advertisement*" in accordance with 18 U.S.C. Section 1734 solely to indicate this fact.

The atomic coordinates and structure factors (code 1FMV/1FMW) have been deposited in the Protein Data Bank, Research Collaboratory for Structural Bioinformatics, Rutgers University, New Brunswick, NJ (http://www.rcsb.org/)..

‡ To whom correspondence should be addressed: Dept. of Biochemistry, 433 Babcock Dr., Madison, WI 53706-1544. Tel.: 608-262-0529; Fax: 608-265-2904; E-mail: ivan_rayment@biochem.wisc.edu.

[1] The abbreviations used are: S1dC, *D. discoideum* myosin II motor domain, residues 1–762; Myosin S1, myosin subfragment-1; P-loop, phosphate binding loop or Walker A Motif; MgATPγS, magnesium adenosine 5′-*O*-thiotriphosphate; PEG, polyethylene glycol; S1dC·MgADP·BeF_x, the beryllium fluoride-ADP complex of *D. discoideum* myosin motor domain; r.m.s., root mean square; nanolog, nonnucleotide analog; AMP-PNP, adenosine 5′-(β,γ-imino)triphosphate.

which was obtained in the presence of MgADP·BeF_x and was similar to that observed in chicken skeletal myosin subfragment-1 (10). The other obtained in the presence of MgADP·AlF_4 and MgADP·VO_4 appeared to represent the conformation of the myosin head in the metastable state (10, 11).

Subsequent studies on the motor domain and myosin head of smooth muscle myosin demonstrated that the structure of the motor domain observed in the complex with MgADP·AlF_4 and MgADP·VO_4 are representative of the conformation of the myosin head at the start of the powerstroke (16). Conversely a more recent structure of scallop myosin subfragment-1 complexed with MgADP revealed a similar conformation of the nucleotide binding pocket, but altered its orientation of the light chain binding motif relative to that seen in any of the other structures (17). Thus the question still remains as to the relationship between the structure observed in chicken skeletal myosin S1 and the contractile cycle.

To address the question of whether the conformation of the motor domain observed in chicken skeletal myosin S1 and *Dictyostelium* myosin S1dC·MgADP·BeFx represents the structure in the rigor conformation, we have determined the structure of S1dC both in its apo state and bound to MgATP to high resolution. This establishes that the conformation seen in S1dC·MgADP·BeF_x is unable to hydrolyze ATP and most likely represents the initial state (pre-hydrolysis) after release of myosin from actin. It also shows that the protein undergoes very small changes in conformation between the apo and ATP-bound states, which may account for the high binding affinity of myosin for ATP.

EXPERIMENTAL PROCEDURES

Protein Purification and Crystallization—The truncated *D. discoideum* myosin II head fragment, which consists of residues 2–762, was prepared as described previously (10) with one exception. To ensure that the final purified S1dC was free of magnesium pyrophosphate (MgPPi) in the active site, 1 mM ATP was used as the final elution buffer instead of MgPPi and was followed by extensive dialysis.

Crystals of apoS1dC were grown by microbatch from 8.0% (w/v) PEG-8000, 50 mM Hepes, pH 7.0, and 1 mM dithiothreitol. The protein concentration in the final droplet was approximately 5.0 mg/ml. The protein/precipitant drops were immediately microseeded by streak-seeding from previous crystallizations and left at 4 °C. Small crystals appeared overnight and grew to maximum dimensions of 0.1 × 0.4 × 0.4 mm^3 over a period of 1 week.

Crystals of the S1dC·MgATP complex were prepared by transferring single crystals of apo·S1dC to a solution containing 15% PEG-8000, 50 mM Hepes, pH 7.0, 50 mM NaCl, 10 mM ATP, and 10 mM $MgCl_2$. The crystals were stored in this solution for 10 min at 4 °C prior to initiating the rapid cooling process.

X-ray Data Collection and Processing—S1dC crystallizes in the space group $P2_12_12$ with final unit cell dimensions of a = 103.5 Å, b = 179.7 Å, c = 54.1 Å (apoS1dC) and a = 104.1 Å, b = 180.4 Å, c = 54.2 Å (MgATP complex). High resolution x-ray data were collected at the Stanford Synchrotron Radiation Laboratory (SSRL) beamline 7–1 with a MAR 30-cm imaging plate detector. Prior to data collection, crystals were transferred stepwise into a cryoprotectant solution containing 15% PEG-8000, 50 mM Hepes, pH 7.0, 25% ethylene glycol, and 300 mM NaCl. The crystals were allowed to stand in this solution for 5 min at which point they were removed to a fresh droplet of cryoprotectant. This procedure was repeated three times to assure no traces of mother liquor remained. The crystals were then picked up in a loop of surgical suture and flash frozen in a stream of cold nitrogen gas (20). The similar protocol was used to freeze the crystals of the S1dC·MgATP complex, except that MgATP was included in every solution. The crystals spent a minimum of 25 min in contact with solutions of MgATP prior to the final step of rapid cooling. Intensity data were processed and scaled with the programs DENZO and SCALEPACK (21). X-ray data processing statistics are presented in Table I.

Structure Determination and Refinement—The atomic coordinates from the isomorphous complex S1dC·MgAMP-PNP (without, MgAMP-PNP, and all solvent molecules, Protein Data Bank accession number 1MMN) (14) were used as an initial model for refinement of both structures. Refinement was carried out with TNT (22) followed by manual model rebuilding with Turbo FRODO (23). At this point $Mg(OH_2)$ATP could be clearly seen in the F_o-F_c electron density map for the ATP complex and was included in the model. For both structures, solvent molecules were added with the PEKPIK program of the TNT package (22) in locations where clear density and geometry consistent with a water molecule were observed. Additional cycles of conjugate gradient least squares were preformed with TNT until convergence was achieved. The quality of the models were assessed with PROCHECK (24) and the PHIPSI program of the TNT package. The final refinement statistics are given in Table II. The x-ray coordinates have been deposited in the Protein Data Bank with file names: apoS1dC, 1FMV and S1dC·MgATP, 1FMW. Root mean square differences (r.m.s.) between coordinates sets were determined with the program ALIGN (25).

TABLE I
X-ray data statistics

Compound	S1dC · MgATP	apoS1dC
Number of crystals used	1	1
Maximum resolution (d_{min}, Å)	2.15	2.10
Total reflections measured to d_{min}	149,338	202,575
Independent reflections to d_{min}	54,467	59,189
R_{merge} (%)[a]	8.3	5.3
Theoretical number of reflections to d_{min}	56,461	59,853
cumulative % completeness	96	99
% completeness in highest resolution shell	95[b]	98[c]
Unit cell parameters	*Å*	
a	104.1	103.5
b	180.4	179.7
c	54.2	54.1

[a] $R = \Sigma|I - \bar{I}|/\Sigma I \times 100$.
[b] 2.23–2.15 Å.
[c] 2.18–2.10 Å.

RESULTS AND DISCUSSION

The three-dimensional structures of the S1dC myosin head from *Dictyostelium* in its apo state and complexed with MgATP were determined to 2.1 and 2.15 Å resolution, respectively. Models contain a total of 743 and 738 amino acid residues of a total of 761 for the apo and MgATP complex, respectively. The electron density for the apo structure is well defined except for three short gaps, Arg^{203}–Gly^{207}, Ile^{500}–Phe^{503}, and Lys^{623}–Asn^{626}. In addition, 20 amino acid residue side chains were disordered and built as alanines (Table II). For apoS1dC, 90.6 and 9.2% of the conformational angles for the mainchain atoms lie in the most favored and additionally favored regions of the Ramachandran plot, respectively. One residue, Thr^{274}, lies outside these regions. Likewise the electron density for the S1dC·MgATP complex is well defined. There are three short gaps in the structure; Arg^{202}–Gly^{207}, Asn^{500}–Leu^{508}, Lys^{623}–Phe^{627}. In addition, 18 amino acid residue side chains were disordered and built as alanines (Table II). In the S1dC·MgATP complex, 90.3 and 9.6% of the residues exhibit conformational angles that lie in the most favored and additionally favored regions of the Ramachandran plot, respectively. Again, Thr^{274} lies outside these regions. The electron density surrounding this residue in both complexes is well defined so there is no obvious reason for its unusual angles.

Structure of S1dC·MgATP—Although the structure of S1dC·MgATP was determined subsequent to that of apoS1dC, this structure is described first because of its relationship to the previously determined nucleotide complexes. As anticipated, MgATP binds in the nucleotide binding pocket defined by the P-loop and the surrounding secondary structural elements (Fig. 1). The electron density for MgATP is well defined (Fig. 2*a*). Examination of the electron density values associated with the γ-phosphate and the temperature factors relative to the other atoms of the nucleotide suggests that exceedingly little hydrolysis has occurred. The structure is very similar to that of S1dC·MgATPγS and S1dC·MgAMP-PNP. The r.m.s. difference between 694 structurally equivalent α-carbons of

TABLE II
Refinement statistics[a]

	S1dC · MgATP	apoS1dC
Resolution limits (Å)	30.0–2.15	30.0–2.10
Final *R*-factor[b]	20.6	19.6
R-free	28.6	28.0
Number of reflections (working set)	52,350	57,680
Number of reflections (test set)	5241	5739
Number of protein atoms	5865	5908
Number of solvent molecules	504	602
Other molecules, ions	1 Mg^{+}, 1 ATP	1 chloride
Average B value-mainchain atoms	42.5	34.8
- all protein atoms	40.5	33.8
- solvent atoms	47.6	42.7
Weighted r.m.s. deviations from ideality		
Bond lengths (Å)	0.014	0.013
Bond angles (°)	2.46	2.68
Planarity (trigonal) (Å)	0.005	0.008
Planarity (others) (Å)	0.007	0.012
Torsional angles (°)	17.9	17.1
Side chains built as alanines	K^{63}, Q^{68}, D^{69}, K^{73}, S^{208}, K^{306}, E^{312}, K^{358}, K^{361}, E^{365}, R^{445}, L489V, K^{498}, D^{505}, F^{506}, K^{622}, K^{661}, K^{670}, P^{714}, D^{715}	K^{62}, Q^{68}, D^{69}, S^{208}, E^{291}, K^{316}, E^{322}, K^{358}, K^{361}, E^{365}, Q^{443}, R^{445}, L489V, K^{498}, K^{622}, K^{661}, K^{670}, K^{728}

[a] TNT refinement.
[b] $R = \Sigma||Fo| - k|Fc|| / \Sigma|Fo|$.

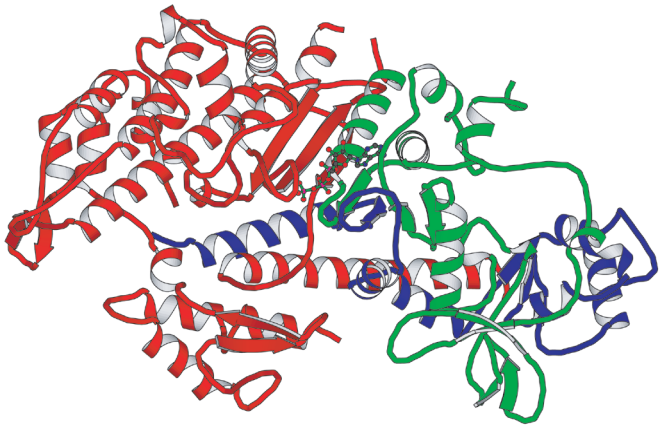

FIG. 1. **Ribbon representation of S1dC·MgATP showing the location of MgATP.** Figs. 1–4 were prepared with the programs Molscript and Bobscript (37, 26).

S1dC·MgATP and S1dC·MgATPγS complexes is 0.21 Å whereas for 718 structurally equivalent α-carbons in S1dC·MgAMP-PNP the r.m.s. difference is 0.16 Å. The coordination of the nucleotides in the binding pocket is remarkably similar (Fig. 3).

Careful examination of the hydrogen bonding pattern surrounding the γ-phosphate in the complexes with MgATP and MgAMP-PNP reveals that there are essentially no differences in the way that the phosphate interacts with the protein. Likewise, apart from the presence of a sulfur atom in MgATPγS, the coordination of the other oxygen atoms is identical to that of MgATP. Most of the water molecules observed in the γ-phosphate binding pocket are common to all these complexes. This raises the question of why MgATP binds so much more tightly to the active site of myosin relative to the commonly used non-hydrolyzable analogs.

Thus far a total of three analogs that closely mimic ATP have been observed bound to *Dictyostelium* S1dC; these include MgATPγS, MgAMP-PNP, and MgADP·BeF_x. Each of these share much in common with MgATP but differs in an important way from the true substrate such that the binding affinity or ability to be hydrolyzed is compromised. In the case of MgAMP-PNP the γ-phosphorous and its three non-bridging oxygen atoms overlap the equivalent atoms of MgATP remarkably well. The difference for MgAMP-PNP arises from the bridging nitrogen between β- and γ-phosphate moieties. This induces the amido side chain of Asn^{233} to rotate to accept a hydrogen bond from the proton on the bridging nitrogen (14). As a consequence, the hydrogen bonding network surrounding the nucleotide is perturbed which accounts for the reduction in its binding affinity for myosin by a factor of at least 10^6 relative to ATP (27).

MgATPγS is broadly considered to be the best analog of MgATP; however, in the case of myosin this compound is slowly hydrolyzed. Even so, MgATPγS binds very tightly to myosin and induces a state where myosin binds weakly to actin. The rate of hydrolysis of MgATPγS is comparable with the steady rate of hydrolysis of ATP (28, 29) but is considerably slower than the actin-activated rate. The rate of hydrolysis of MgATPγS is not enhanced by actin (28, 29), which suggests that the metastable state is not attained for ATPγS and that the rate-limiting step for hydrolysis of this nucleotide is bond cleavage rather than product release as for ATP. Comparison of the structures of S1dC·MgATP and S1dC·MgATPγS reveals that all of the atoms of these nucleotides superimpose exceedingly well and only differ for the terminal sulfur atom on ATPγS (Fig. 3). Interestingly the oxygen of ATP that falls in the same location as the sulfur atom of ATPγS forms an ionic interaction with Nζ of Lys185 and hydrogen bonds to two solvent molecules. A similar ionic interaction is formed by Sγ of ATPγS; however, as might be expected there are no well defined hydrogen bonds to solvent molecules. In both cases, the oxygen of ATP and sulfur of ATPγS face toward the apex of the cleft that splits the 50-kDa region of the myosin heavy chain, which may account for the small penalty in reduced binding affinity by the replacement of an oxygen by a sulfur.

Structural comparison of MgATP to MgADP·BeF_x is more complex because of the ill defined nature of the exact metallo-hydroxyfluoride species bound in the active site (30). As shown in Fig. 3, the positions of the fluorines or hydroxyl groups are very close to those of the terminal oxygens of ATP. This con-

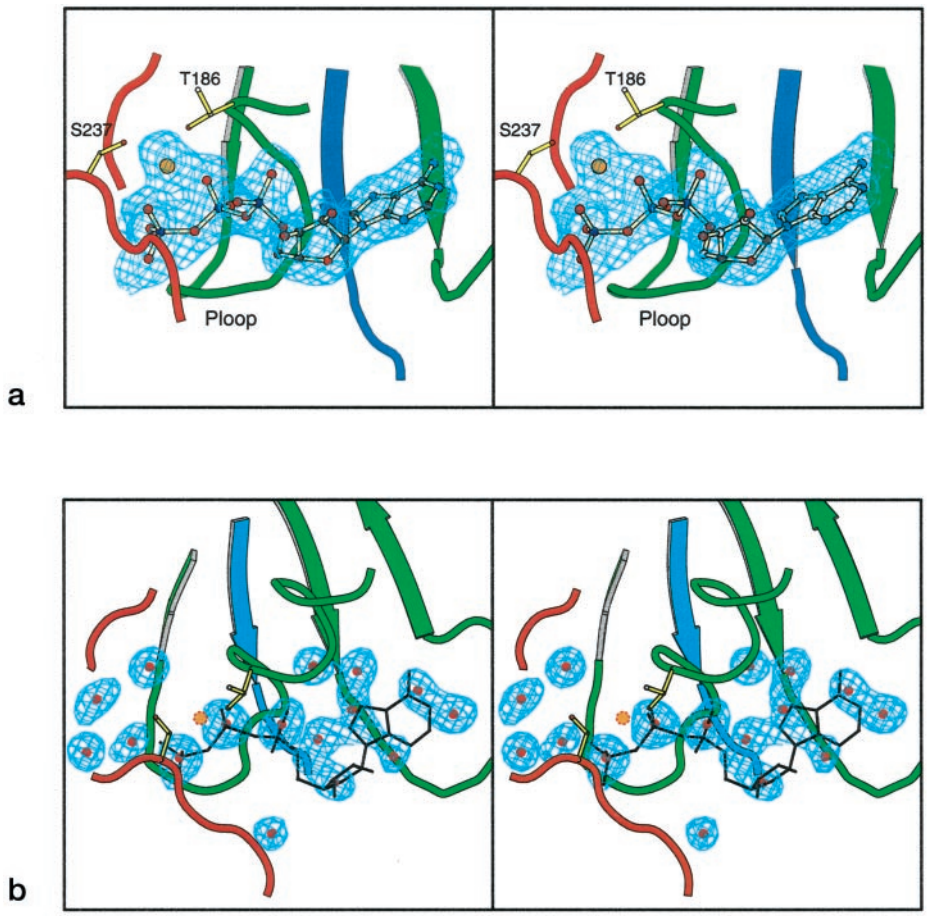

FIG. 2. **Stereoview of the difference density for MgATP (*a*) and the solvent electron density in apoS1dC (*b*).** The location of ATP is shown superimposed on the solvent structure for the apoS1dC. The coefficients used in the calculation were of the form F_o-F_c where the substrate and water molecules were removed from the refinement.

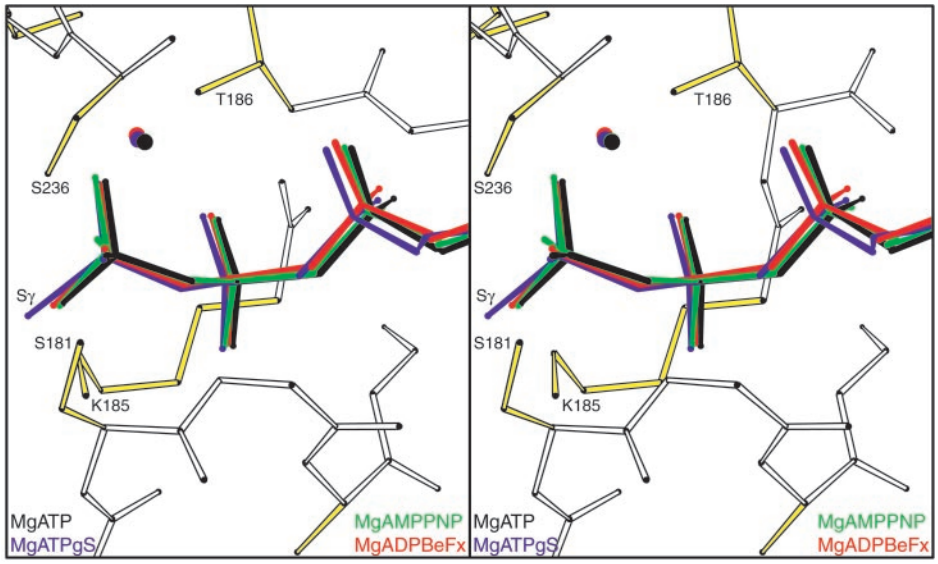

FIG. 3. **Stereoverlap of the triphosphate-like moiety of MgATP (*black*), MgATPγS (*dark blue*), MgAMP-PNP (*green*), and MgADP·BeF_x (*red*).** The coordinates of each of these complexes were superimposed with the program ALIGN (25) modified at the University of Wisconsin by Gary Wesenberg to allow selection of the segments used for alignment (available on request). The alignment was based on the α-carbons surrounding the nucleotide and consisted of residues 174–184, 235–245, and 450–455.

firms that MgADP·BeF_x is a good structural analog of MgATP in that it serves to trap myosin in a conformation induced by the true substrate. Biochemical evidence suggests that MgADP·BeF_x is more closely related to the pre-hydrolysis complex with ATP than the metastable state (31–33). Formation of the MgADP·BeF_x complex is sufficient to lower the binding affinity of myosin for actin (34). However, the complex with beryllium fluoride differs from the true substrate in that it is unable to induce the metastable state of myosin in solution and hence cannot drive the contractile cycle. Even so, it is a potent

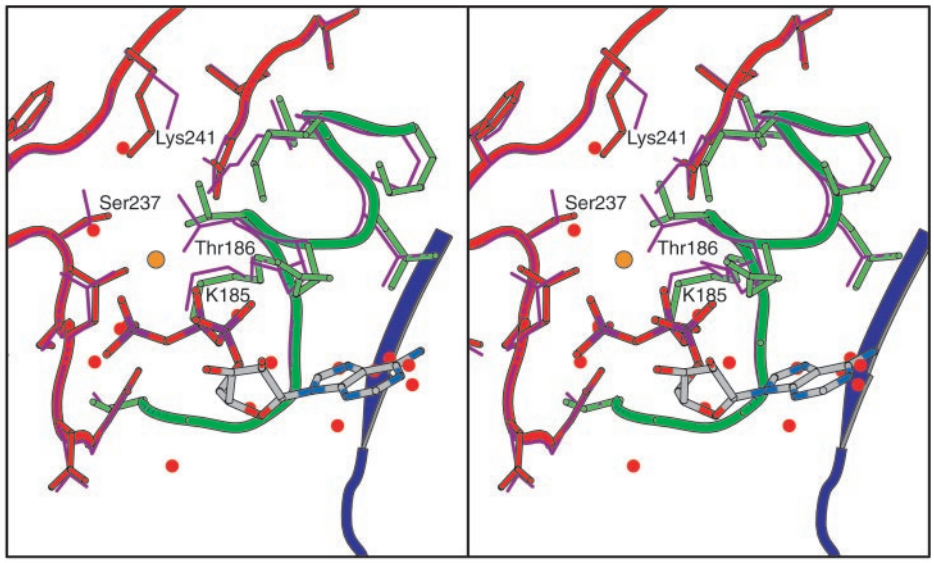

FIG. 4. **Stereoview of nucleotide binding pockets of apoS1dC and S1dC·MgATP showing the similarity in the side chains that line the active site.** The protein side chains of S1dC·MgATP are depicted in *green* and *red*, whereas the equivalent residues in apoS1dC are shown as *thin purple lines*. The water molecules in apoS1dC are depicted as *red spheres*. MgATP is shown in *stick-representation* where the atoms are colored according to their atom type. This shows a comparison of the water structure in the apoS1dC with adenosine in S1dC·MgATP.

inhibitor of the ATPase activity in solution, which suggests that there is a small conformational difference in free energy of the protein between the structure of myosin in solution and that bound to MgATP. This is confirmed by the structure of apoS1dC described below.

Structure of ApoS1dC—Remarkably, the structure of apoS1dC is very similar to that of S1dC when co-crystallized with a variety of nucleotide analogs that mimic ATP. The r.m.s. difference between apoS1dC and S1dC·MgATPγS and S1dC·MgADP·BeF_x is 0.31 and 0.53 Å, respectively for 729 and 734 structurally equivalent α-carbons. Similarly, binding of MgATP to crystalline apoS1dC does not induce any major conformational changes as indicated by the r.m.s. difference between 725 α-carbons of 0.28 Å. The structure of apoS1dC is also very similar to that of chicken skeletal myosin subfragment-1 where the r.m.s. difference between 603 structurally equivalent α-carbons is 1.13 Å.

In addition to the similarity of the overall folds of the apo and ATP structures, the orientation of the ligands that coordinate the nucleotide are also remarkably similar. The only small changes are rotation of the side chains associated with the metal binding pocket in the nucleotide complexes, including Thr^{186}, Ser^{237}, and Lys^{241} (Fig. 4). There are also small movements of the side chains that interact with the adenine ring. Of these, only the movement of Ser^{237} and Thr^{186} are significant and even these simply reflect rearrangements to accommodate the absence of a metal ion and allow new interactions with the solvent molecules. The other small differences in the orientation of ligands that surround the nucleotide binding pocket are similar to those seen between the other complexes determined to date.

The nucleotide binding pocket is occupied by more than 11 solvent molecules (Figs. 2*b* and 4). Interestingly the constellation of ordered water molecules approximate the hydrogen bonding potential of ATP. For example, there is a water molecule located at the approximate location of each phosphate, the ribose ring oxygen, and also at the N1, N7 and N10 positions of the purine ring. Outside the water molecules that take up the space otherwise occupied by the nucleotide, the solvent structure in the nucleotide binding pocket is very similar to that seen in the S1dC complexes MgATP, MgATPγS, and other analogs. This again emphasizes the role that the water structure plays in coordination of ATP as noted previously in the study of the interaction of non-nucleotide analogs with myosin (15).

The remarkable similarity between the active site in the presence and absence of ATP accounts for, in part, the very high binding affinity of myosin for ATP. It is clear that very little of the binding energy of myosin for ATP is devoted toward changing the conformation of the protein. Even the water structure is conserved in the apo structure. Conservation of the protein and water structure would appear to reduce the entropic cost of coordinating the substrate in the active site.

Conclusions—The structures of apoS1dC and S1dC·MgATP reveal two important pieces of information about myosin. First, the overall structure of apoS1dC is very similar to those obtained by co-crystallizing the protein in the presence of the nonhydrolyzable analogs of ATP and second, when myosin is in this conformation it does not hydrolyze MgATP. Whereas the close similarity between the apo and nucleotide-bound states explains the high binding affinity of myosin for MgATP it comes as a surprise that MgATP is stable within the crystal lattice. This is a critical observation because in solution, the protein is fully active and would be expected to turn over the nucleotide within the time frame of the experiment (35, 36). The most likely explanation is that the conformation observed here is unable to hydrolyze MgATP. This hypothesis was proposed previously on the basis of the studies with S1dC·MgATPγS, which when co-crystallized with the nucleotide analog showed no evidence of hydrolysis (14). In the latter case it could have still been argued that MgATPγS does not have the correct hydrogen bonding pattern around the γ-phosphate and might not bind in a conformation induced by MgATP. This argument cannot be applied to the present structure. The conclusion appears to be that the conformation observed in the S1dC·MgATP complex and also in chicken skeletal myosin subfragment-1 is one of the pre-hydrolysis states available to myosin in solution. Evidence for additional states in solution are provided by the structure of scallop myosin that shows a different orientation of the converter domain even though the conformation around the γ-phosphate binding pocket is very similar (17).

Although it is possible that the structures seen here are unique to *Dictyostelium* and the particular fragment under

investigation, it is unlikely because the conformation of the 50-kDa domains are very similar in chicken S1 and scallop S1. Rather, it suggests that the open conformation of the motor domain is a state that will belong to all pre-hydrolyis states. The present study refutes any proposals that the conformation of chicken skeletal myosin subfragment-1 belongs to the rigor state. However, because the structure of chicken skeletal myosin subfragment-1 approximately fits into image reconstructions of actomyosin, it seems more likely that this conformation represents the state of myosin shortly after its release from actin. This work does not conflict with the smooth muscle ADP·BeF_x structure, which adopts the closed conformation. The metastable state must be able to accommodate both MgATP and MgADP-P_i. It should not be surprising that under some crystallization conditions the closed conformation is found in the presence of a MgATP analog. The question remains however, if MgATP were introduced into a crystal that exhibits the closed conformation, would it be hydrolyzed in the lattice.

Acknowledgment—We thank Dr. Andrew M. Gulick for helpful discussions.

REFERENCES

1. Mermall, V., Post, P. L., and Mooseker, M. S. (1998) *Science* **279,** 527–533
2. Sellers, J. R. (2000) *Biochim. Biophys. Acta* **1496,** 3–22
3. Lymn, R. W., and Taylor, E. W. (1971) *Biochemistry* **10,** 4617–4624
4. Dantzig, J. A., and Goldman, Y. E. (1985) *J. Gen. Physiol.* **86,** 305–327
5. Irving, M., St. Claire Allen, T., Sabido-David, C., Craik, J. S., Brandmeier, B., Kendrick-Jones, J., Corrie, J. E., Trentham, D. R., and Goldman, Y. E. (1995) *Nature* **375,** 688–691
6. Baker, J. E., Brust-Mascher, I., Ramachandran, S., LaConte, L. E., and Thomas, D. D. (1998) *Proc. Natl. Acad. Sci. U. S. A.* **95,** 2944–2949
7. Ramachandran, S., and Thomas, D. D. (1999) *Biochemistry* **38,** 9097–9104
8. Brust-Mascher, I., LaConte, L. E., Baker, J. E., and Thomas, D. D. (1999) *Biochemistry* **38,** 12607–12613
9. Rayment, I., Rypniewski, W. R., Schmidt-Bäse, K., Smith, R., Tomchick, D. R., Benning, M. M., Winkelmann, D. A., Wesenberg, G., and Holden, H. M. (1993) *Science* **261,** 50–58
10. Fisher, A. J., Smith, C. A., Thoden, J., Smith, R., Sutoh, K., Holden, H. M., and Rayment, I. (1995) *Biochemistry* **34,** 8960–8972
11. Smith, C. A., and Rayment, I. (1996) *Biochemistry* **35,** 5404–5417
12. Smith, C. A., and Rayment, I. (1995) *Biochemistry* **34,** 8973–8981
13. Bauer, C. B., Kuhlman, P. A., Bagshaw, C. R., and Rayment, I. (1997) *J. Mol. Biol.* **274,** 394–407
14. Gulick, A. M., Bauer, C. B., Thoden, J. B., and Rayment, I. (1997) *Biochemistry* **36,** 11619–11628
15. Gulick, A. M., Bauer, C. B., Thoden, J. B., Pate, E., Yount, R. G., and Rayment, I. (2000) *J. Biol. Chem.* **275,** 398–408
16. Dominguez, R., Freyzon, Y., Trybus, K. M., and Cohen, C. (1998) *Cell* **94,** 559–571
17. Houdusse, A., Kalabokis, V. N., Himmel, D., Szent-Gyorgyi, A. G., and Cohen, C. (1999) *Cell* **97,** 459–470
18. Rayment, I., Holden, H. M., Whittaker, M., Yohn, C. B., Lorenz, M., Holmes, K. C., and Milligan, R. A. (1993) *Science* **261,** 58–65
19. Holmes, K. C. (1997) *Curr. Biol.* **7,** R112–118
20. Rodgers, D. W. (1997) *Methods Enzymol.* **276,** 183–203
21. Otwinowski, Z., and Minor, W. (1997) *Methods Enzymol.* **276,** 307–326
22. Tronrud, D. E. (1997) *Methods Enzymol.* **277,** 306–319
23. Roussel, A., and Cambillau, C. (1991) *Silicon Graphics Geometry Partners Directory,* Vol. 86, Silicon Graphics
24. Laskowski, R. A., MacArthur, M. W., Moss, D. S., and Thornton, J. M. (1993) *J. Appl. Crystallogr.* **26,** 283–291
25. Cohen, G. H. (1997) *J. Appl. Crystallogr.* **30,** 1160–1161
26. Esnouf, R. M. (1999) *Acta Crystallogr. Sec. D* **55,** 938–940
27. Greene, L. E., and Eisenberg, E. (1980) *J. Biol. Chem.* **255,** 543–548
28. Goody, R. S., and Mannherz, H. G. (1975) in *Protein-Ligand Interactions* (Sund, H., and Blauer, G., eds) pp. 109–127, de Gruyter, Berlin
29. Resetar, A. M., and Chalovich, J. M. (1995) *Biochemistry* **34,** 16039–16045
30. Henry, G. D., Maruta, S., Ikebe, M., and Sykes, B. D. (1993) *Biochemistry* **32,** 10451–10456
31. Ponomarev, M. A., Timofeev, V. P., and Levitsky, D. I. (1995) *FEBS Lett.* **371,** 261–263
32. Phan, B. C., Cheung, P., Stafford, W. F., and Reisler, E. (1996) *Biophys. Chem.* **59,** 341–349
33. Park, S., Ajtai, K., and Burghardt, T. P. (1997) *Biochemistry* **36,** 3368–3372
34. Rostkova, E. V., Moiseeva, L. N., Teplova, M. V., Nikolaeva, O. P., and Levitsky, D. I. (1999) *Biochemistry* (*Mosc*) **64,** 875–882
35. Itakura, S., Yamakawa, H., Toyoshima, Y. Y., Ishijima, A., Kojima, T., Harada, Y., Yanagida, T., Wakabayashi, T., and Sutoh, K. (1993) *Biochem. Cell Biol.* **196,** 1504–1510
36. Kurzawa, S. E., Manstein, D. J., and Geeves, M. A. (1997) *Biochemistry* **36,** 317–323
37. Kraulis, P. J. (1991) *J. Appl. Crystallogr.* **24,** 946–950